Characterization of Two Important Histidine Residues in the Active Site of Xylanase A from *Streptomyces lividans*, a Family 10 Glycanase[†]

M. Roberge, F. Shareck, R. Morosoli, D. Kluepfel, and C. Dupont*

Centre de recherche en microbiologie appliquée, Institut Armand-Frappier, Université du Québec, Laval, Québec, Canada H7N 4Z3

Received February 13, 1997; Revised Manuscript Received April 14, 1997[⊗]

ABSTRACT: The active site of xylanase A (XlnA) from *Streptomyces lividans* contains three histidine residues, two of which (H81 and H207) are almost completely conserved in family 10 glycanases. The structural analysis of the enzyme shows that H81 and H207 are part of an important hydrogen bond network in the vicinity of the two catalytic residues (E128 and E236). In order to investigate the role of these two histidine residues for the structure/function of XlnA, three mutant enzymes were produced at each position, namely, H81R/S/Y and H207E/K/R. The specific activity of these mutant enzymes is reduced by more than 95%, revealing the importance of these two residues for the catalytic function of XlnA. The kinetic parameters of the three more active enzymes were determined, of which mutation H207K increased the K_M 3-fold. The k_{cat} of the mutant enzymes is reduced proportionally to the specific activity. Furthermore, the pK_a values of the two catalytic residues are decreased in all six mutations, demonstrating a role for H81 and H207 in the hydrogen bond network responsible for maintaining the ionization state of the two catalytic residues. In most cases, the unfolding of mutated XlnA in guanidine hydrochloride (Gdn-HCl) showed that the concentration required to denature 50% of the XlnA decreased, thus demonstrating the importance of those two residues for the stability of the enzyme. Moreover, the *m* value [$m = d(\Delta G)/d[\text{Gdn-HCl}]$] for the unfolding of XlnA in Gdn-HCl is increased for each of the six mutations, suggesting that the mutant proteins have less residual structure in the denatured state than does the wild-type enzyme.

Xylanases are classified into two distinct families of glycosyl hydrolases according to their primary structure (families 10 and 11) (*1*). *Streptomyces lividans* produces three xylanases, xylanase A (XlnA)[1] belonging to family 10 and xylanases B and C which belong to family 11. Three-dimensional structures of xylanases from both families have been elucidated, and they show a completely different fold. All known structures of family 10 xylanases fold in a $(\alpha/\beta)_8$ barrel (*2, 3, 4, 5*) while xylanases from family 11 are composed mainly of β-sheets (*6, 7, 8, 9*). Xylanases from family 10 also belong to the 4/7 superfamily of glycosyl hydrolases which includes several hydrolase families with various substrate specificities (*10, 11, 12*).

While xylanases from families 10 and 11 have very different overall structures, they use the same double displacement mechanism for the hydrolysis of the xylosidic bond. Xylanases hydrolyze β-1,4 bonds in an endo fashion with net retention of the configuration of the anomeric carbon. This mechanism involves two carboxylic catalytic residues: the acid/base catalyst, which is protonated for the glycosylation step, and a nucleophile, which is ionized for the stabilization of the oxocarbonium intermediate (*13*). In XlnA, these two catalytic residues were identified by site-directed mutagenesis as E128 and E236, respectively (*14*). The three-dimensional structure of XlnA corroborates these assignments and suggests that other amino acids may form an important network of hydrogen bonding in the vicinity of the glutamic acid residues. More specifically, in XlnA from *S. lividans*, H81 and H207 are in close proximity to and are involved in hydrogen bonding with E236, the nucleophile (*2*). The corresponding histidine residues in other xylanases of family 10 have also been shown to be involved in interactions with their nucleophile.

The three-dimensional structure of Cex from *Cellulomonas fimi*, a family 10 xylanase, reveals an important hydrogen bonding network in the active site, implicating one histidine residue (H205) (corresponding to H207 of *S. lividans* XlnA) that is responsible for maintaining the ionization state of the nucleophile (*3*). This structure, and the results of site-directed mutagenesis experiments, suggests the involvement of H80 (corresponding to H81 of *S. lividans* XlnA) in substrate recognition (*3*). These histidine residues were also suggested to be involved in maintaining the ionization state of the nucleophile in two other family 10 xylanases (*4, 5*). The structure of the cocrystal of XynA from *Pseudomonas fluorescens* subsp. *cellulosa* with xylopentaose allowed the identification of six subsites (A−F) involved in substrate binding. The enzyme hydrolyzes the β-1,4-xylosidic bond between subsites D and E, which include the two catalytic residues (*4*). By sequence homology, H81 and H207 would be part of subsites E and D, respectively, with H81 interacting with the saccharide moiety present in subsite E.

[†] This work was supported by grant from the Natural Sciences and Engineering Research Council of Canada (NSERC) and by the Fonds pour la formation de chercheurs et l'aide à la recherche du Québec (FCAR), and by a scholarship to M.R. from the Fondation Armand-Frappier.

* To whom correspondence should be addressed. Telephone: 514 687-5010. Fax: 514 686-5501. E-mail: claude_dupont@iaf.uquebec.ca.

[⊗] Abstract published in *Advance ACS Abstracts,* June 1, 1997.

[1] Abbreviations: CD, circular dichroism; Gdn-HCl, guanidine hydrochloride; SDS−PAGE, sodium dodecyl sulfate−polyacrylamide gel electrophoresis; XlnA, *Streptomyces lividans* xylanase A.

S0006-2960(97)00329-2 CCC: $14.00

In this paper, we used site-directed mutagenesis to characterize the function of the two histidine residues (H81 and H207) conserved in family 10 hydrolases that are in the vicinity of the nucleophile E236 of XlnA. To study the role of H81, amino acids capable of hydrogen bonding were chosen to replace histidine, and in the case of H207, histidine was replaced by charged residues to study its involvement in the ionization state of the two catalytic residues. We report the characterization of six mutant proteins at those two positions (H81R/S/Y and H207E/K/R).

MATERIALS AND METHODS

Site-Directed Mutagenesis. Site-directed mutagenesis of the *xln*A gene was performed according to Kunkel (*15*) on phagemid pIAF217 or pAM19.1 (*14*). The following oligonucleotides were used for mutagenesis: H81R, 5′-GGCCAGGGTGCGGCCGCGCAC-3′; H81S, 5′-GGCCAGGGTGCTGCCGCGCAC-3′; H81Y, 5′-CAGGGTGTAGCCGCG-3′; H207E, 5′-GCCGCTGTTGAACTCCGACTGGAA-3′; H207K, 5′-GCTGTTGAACTTCGACTGGAA-3′; and H207R, 5′-GCTGTTGAAGCGCGACTGGAA-3′ [underlining indicates the substituted nucleotide(s)] and were synthesized on a Gene Assembler (Pharmacia). Screening and subcloning of the mutated gene from pIAF217 into plasmid pIAF18 were done as described previously (*14*). The mutated *Sph*I−*Bam*HI fragment from pAM19.1 was cloned directly into pIJ702 (*16*) digested with *Sph*I−*Bgl*II to form the new plasmid pIAF18.1.

Enzyme Production and Purification. XlnA was produced as described (*17*). Proteins contained in the supernatant of *S. lividans* culture were first concentrated by ultrafiltration with a 3 kDa cutoff membrane (Omega). The concentrated proteins were then precipitated with 65% saturation of ammonium sulfate, and after centrifugation, the precipitate was dissolved in 50 mM sodium citrate buffer, pH 6.0. Samples of 100 mg of protein were then loaded on a phenyl-Sepharose column (Pharmacia) in 50 mM sodium citrate buffer containing 1 M ammonium sulfate, pH 5.6. Proteins were eluted with a decreasing linear gradient to 0 M ammonium sulfate, followed by an increasing linear gradient to 50% ethylene glycol. The XlnA-containing fractions were pooled, dialyzed against Milli-Q water, and freeze-dried. The second step consisted of separation on a Superdex HR75 beaded column (3 × 60 cm; Pharmacia) with 100 mM sodium citrate, pH 6.0, as the eluant. The purified XlnA-containing fractions were pooled, dialyzed, and freeze-dried.

Protein Analysis. Protein concentration was determined according to Lowry *et al*. (*18*) using bovine serum albumin as the standard (Bio-Rad). Determination of protein purity was assessed by SDS−PAGE (*19*) and Western blot analysis with anti-XlnA antibodies according to Towbin *et al.* (*20*).

Enzymatic Determinations. The specific activity was determined by incubating the enzymes with 4.5 mg/mL birchwood xylan (Sigma) in 50 mM sodium citrate buffer, pH 6.0, at 60 °C for 10 min. The released reducing sugars were detected using *p*-hydroxybenzoic acid hydrazide (*21*) with an adaptation for microtiter plates. For the determination of Michaelis−Menten constants, the initial velocities of the enzymes were measured at 60 °C in 50 mM sodium citrate buffer, pH 6.0, by using birchwood xylan at increasing concentrations from 0.045 to 4.5 mg/mL. The enzyme concentrations used for wild-type XlnA, H81S, H207K, and H207R were 0.0148, 0.143, 0.639 and 0.696 μM, respectively; higher enzyme concentrations were used for mutant enzymes to compensate for their low activity. The kinetic parameters were calculated with the software EnzFitter ver. 1.03 (*22*). The optimum temperature profiles of the enzymes were determined by measuring the specific activity in 50 mM sodium citrate buffer, pH 6.0, at temperatures ranging between 35 and 80 °C. The pH profiles of hydrolysis were determined by measuring the specific activity of the enzymes in 50 mM phosphate buffer at pH values ranging from 4.0 to 9.0. The pK_a values of the catalytic groups were determined in subsequent experiments. The initial velocities of the enzymes (k_{cat} apparent) were determined at a xylan concentration of 48K_M in 50 mM sodium phosphate buffer at pH values of 4.0 to 10.5. The pK_a values corresponding to the enzyme−substrate complex were determined from the plot of k_{cat} apparent *vs* pH using the software GraFit ver. 3.09b (*23*).

Stability of the Enzyme. For the determination of the stability, solutions of 500 μg/mL enzyme were incubated at 60 °C. Samples were removed at various time points for the determination of residual activity. The half-lives were obtained by plotting the natural logarithm of the residual activity as a function of time of incubation. Stability was determined in the presence of substrate by incubating the enzyme with 7.2 mg/mL birchwood xylan in 50 mM sodium citrate buffer, pH 6.0. At various times, aliquots were withdrawn and analyzed for their content of reducing sugars. The XlnA half-lives were determined by nonlinear analysis of time versus released reducing sugars plots.

Circular Dichroism (CD). Solutions of 500 μg/mL xylanase in 10 mM sodium phosphate buffer, pH 6.0, were analyzed at room temperature using a 0.5 mm jacketed cell on a Jasco J-710 spectropolarimeter interfaced with an IBM computer. Data were averaged from 10 acquisitions between 250 and 184 nm at a scan rate of 100 nm/min. Samples for tertiary structure changes were analyzed in a 1 cm cell between 350 and 240 nm under the same conditions. Denaturation curves were obtained with solutions containing 0.2 mg/mL xylanase and increasing concentration of Gdn-HCl in 10 mM sodium phosphate buffer, pH 6.0. Samples were incubated for 24 h at 25 °C prior to CD analysis, and five measurements at 285.2 nm in a 1.0 cm cell were taken and averaged. These values were then transformed into the fraction of unfolded protein according to eq 1 assuming a two-state unfolding mechanism:

$$f_U = (X - X_n)/(X_U - X_n) \quad (1)$$

where X_n is the value of the native protein, X_U the value for the unfolded protein, and X the value observed. Data in the transition of the f_U *vs* [Gdn-HCl] plot were transformed to calculate the standard free energy of unfolding (ΔG) according to eq 2 (*24*):

$$\Delta G = \Delta G(H_2O) - m[\text{Gdn-HCl}] \quad (2)$$

where $\Delta G = -RT \ln [(X_N - X)/X - X_U)]$, $\Delta G(H_2O)$ is the ΔG extrapolated at 0 M Gdn-HCl from the ΔG vs [Gdn-HCl] plot, and $m = d(\Delta G)/d[\text{Gdn-HCl}]$.

RESULTS

The specific activity is greatly reduced by the mutations introduced at positions 81 and 207 of XlnA. Losses of 99.8,

Table 1: Specific Activity and Kinetic Parameters of Wild-Type and Mutant Xylanases Using Birchwood Xylan as the Substrate

enzymes	sp act. (IU·mg^{-1})	K_M (mg·mL^{-1})	k_{cat} (s^{-1})
wild-type	174	0.10	134
H81R	0.3	*a*	*a*
H81S	8.4	0.10	6.6
H81Y	0.5	*a*	*a*
H207E	0.7	*a*	*a*
H207K	1.9	0.31	1.6
H207R	1.3	0.10	0.9

[a] Parameters not determined.

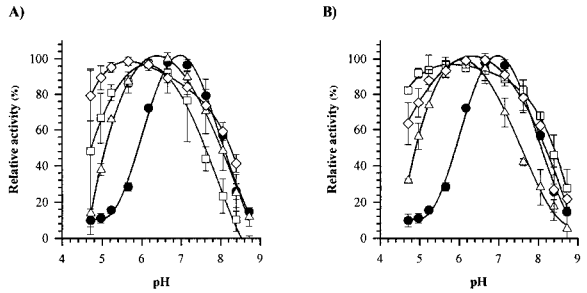

FIGURE 1: pH profiles of wild-type (closed circles) and mutant (open symbols) xylanases. Panel A: H81 mutant enzymes (H81R, squares; H81S, triangles; H81Y, diamonds) Panel B: H207 mutant enzymes (H207E, squares; H207K, triangles; H207R, diamonds).

95.2, and 99.7% are observed for H81R/S/Y, respectively, while H207E/K/R mutations cause a decrease of 99.6, 98.9, and 99.3%, respectively (Table 1). However, the mutant enzymes H81S, H207K, and H207R retained sufficient activity to determine their kinetic parameters on birchwood xylan. While the conditions used for the determination of the kinetic parameters were optimal for wild-type XlnA, they were sufficiently close to those of the mutants so that the parameters could be compared. The k_{cat} values are affected in proportions similar to the decrease in specific activity. The affinity for birchwood xylan (K_M) is changed only in the case of H207K, which exhibits a K_M value 3 times higher than that of the wild-type enzyme (Table 1).

The optimum temperature profile of XlnA was not affected significantly by any of the mutations, being 60 °C under standard conditions (data not shown). The pH profiles of the modified enzymes were determined and compared to that of the wild-type enzyme (Figure 1). For all mutations at positions H81 and H207, the pH profile is shifted toward acid pH. In the cases of H81R and H207K, the pH profile is also affected on the alkaline side, but to a lesser extent. Thus, the postulated effect of the different mutations on the ionization state of the two catalytic glutamic acid residues was verified. To minimize the influence of enzyme stability on the pH profile, the pH dependence of k_{cat} was determined in order to measure accurately the pK_a of the two catalytic residues. McIntosh *et al*. (*25*) have shown, by using nuclear magnetic resonance, that the two breaks in the pH profile of *Bacillus circulans* xylanase (family 11) were caused by changes in the ionization state of the nucleophile and the acid/base catalyst. For wild-type XlnA, pK_a values of 4.82 and 9.40 were obtained for the nucleophile and acid/base catalyst, respectively, and were similar to those found for other 4/7 superfamily members (*26*). In all cases, the apparent pK_a of the two catalytic residues is shifted toward acidic pH. For the six mutations studied, the calculated pK_a shifts are 0.21−0.85 pH unit for the nucleophile glutamic acid and 0.33−0.59 pH unit for the acid/base catalyst residue (Table 2).

Table 2: pK_a Values of the Catalytic Residues for XlnA and Mutants Enzymes

	pK_a value [a]	
enzyme	nucleophile E236	acid/base catalyst E128
wild-type	4.82 ± 0.01	9.40 ± 0.02
H81R	4.03 ± 0.05	8.95 ± 0.05
H81S	3.97 ± 0.24	9.07 ± 0.23
H81Y	4.26 ± 0.18	8.97 ± 0.20
H207E	4.24 ± 0.10	8.81 ± 0.10
H207K	4.61 ± 0.07	8.95 ± 0.09
H207R	4.19 ± 0.06	8.90 ± 0.06

[a] Calculated from k_{cat} vs pH plot using Grafit ver. 3.09b software (Leatherbarrow, 1990).

In comparison to the wild-type enzyme, all mutations reduce the enzyme's stability at 60 °C at least 75% in the absence of substrate (Table 3). In the presence of xylan, the protein is protected from denaturation at this temperature. All mutations at position H81 (H81R/S/Y) have half-lives comparable to the wild-type (318 min). Among those at position H207, H207E and H207K have half-lives in the same range (312 and 234 min, respectively), whereas the half-life of H207R is considerably shorter (84 min, Table 3).

The stability of the mutant proteins was also assessed by CD by determining the unfolding curve of each enzyme in Gdn-HCl (Figure 2), and the unfolding transition midpoints of all mutants were compared to that of the wild-type enzyme. Only the H81Y mutation did not destabilize XlnA, while mutations H81R/S slightly decrease the unfolding transition midpoint from 1.98 M to 1.72 and 1.89 M, respectively (Table 3). Mutations at position H207 have a greater destabilizing effect on XlnA. The unfolding midpoint is decreased by 0.77, 0.59, and 0.70 M for mutation H207E/K/R, respectively (Table 3). Mathematical transformation of the data from the unfolding curves allows the calculation of two other parameters: the *m* value, which reflects the sensitivity of the ΔG of unfolding in relation to Gdn-HCl concentration; and the $\Delta G(H_2O)$, which represents the difference in free energy between the native and the denatured state of the protein extrapolated to 0 M Gdn-HCl. All six mutations significantly increase the *m* value for Gdn-HCl (Table 3). This result is unexpected for single point mutations. These increased *m* values result in higher standard free energies of unfolding for five out of six mutants; only H207K has a $\Delta G(H_2O)$ comparable to that of the wild-type enzyme (Table 3).

The mutated enzymes show typical mobility on SDS−PAGE and reacted with anti-XlnA antibodies in Western blot analysis (data not shown). Comparison of their far-UV spectra by circular dichroism with the wild-type protein shows that the mutations introduced at positions 81 and 207 did not greatly affect the overall structure of the protein. This suggests that the kinetic and stability variations observed were not due to any major change in the three-dimensional structure of the mutant proteins as minor structural changes may not be detected by CD (Figure 3).

DISCUSSION

Xylanase A from *Streptomyces lividans* contains six histidine residues, three of which are located in the active

Table 3: Stability Parameters of the Modified Xylanases

enzymes	half-life (min) without substrate	half-life (min) with substrate	Denaturation transition midpoint, [Gdn-HCl] (M)	m value[a] (kJ mol^{-1} M^{-1})	standard free energy of unfolding, $\Delta G(H_2O)$ (kJ·mol^{-1})
wild-type	131	318 ± 42	1.98	4.90	9.7
H81R	33	360 ± 60	1.72	9.94	17.1
H81S	17	276 ± 60	1.89	7.25	13.7
H81Y	27	300 ± 54	1.99	6.58	13.1
H207E	24	312 ± 30	1.21	9.50	11.5
H207K	5	84 ± 12	1.39	6.99	9.7
H207R	10	234 ± 42	1.28	14.45	18.5

[a] Calculated from eq 2.

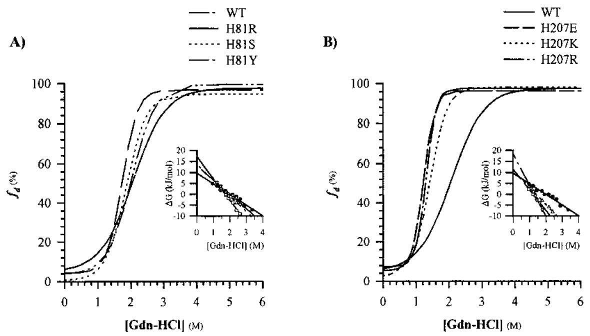

FIGURE 2: Denaturation curves in Gdn-HCl of wild-type and mutant xylanases A. Panel A: H81 mutants. Panel B: H207 mutants. Inset: Data in the transition were transformed as described under Materials and Methods to plot the variation of ΔG as a function of [Gdn-HCl].

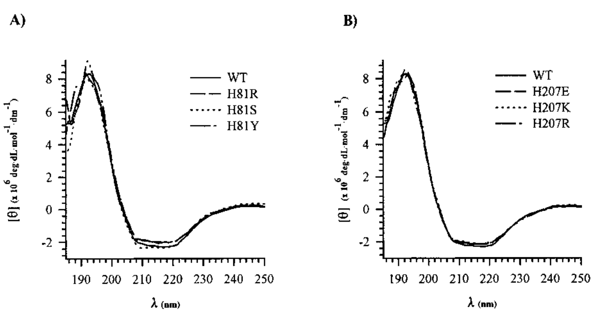

FIGURE 3: Circular dichroism spectra of wild-type and mutant xylanases. Panel A: H81 mutants. Panel B: H207 mutants.

site of the enzyme. Primary sequence analysis of xylanases belonging to family 10 shows that H81 and H207 are invariant in all but one case (Figure 4). Moreover, these two histidines are part of the eight conserved amino acids identified for superfamily 4/7 (*26*). The elucidation of the role of these histidine residues in XlnA will contribute to the understanding of the importance of the hydrogen-bonding network in the vicinity of the active site for the structure/function of glycosyl hydrolases belonging to this superfamily.

The three-dimensional structure of XlnA shows that H207 (Nϵ2) is hydrogen-bonded to E236 (Oϵ2) and that its Nδ1 atom is bonded to D238 (Oδ2) (Figure 5). E236 and D238 are part of the conserved ITELDI motif found in xylanases belonging to family 10. This suggests that the interaction of H207 with this conserved structural feature of family 10 glycanases may be important for the structure/function of these enzymes. The three mutations introduced at position 207 almost abolish the enzyme activity, confirming the crucial role of this amino acid for efficient catalysis. The activity of the mutant proteins was generally sufficient for further characterization. However, when the specific activity was less than 1 IU/mg, it was impossible to determine the

```
                  ▼    ▼                                ▼
SlivA   121-GHTLAWHS..QQPGW-133    239-PIDCVGFQSHFNSG..SPYN-256
Acti2   118-GHTLAWHS..QQPGW-130    236-PIDCVGFQSHFNSG..SPYN-253
AawaA   108-GHTLVWHS..QLPSW-120    226-PIDGIGSQTHLSAGGGAGIS-245
BaccA   130-FHTLVWHS..QVPEW-142    263-PIDGVGHQSHIQI.GWPSI.-280
BsteA   121-FHTLVWHS..QVPQW-134    255-PIDGIGHQSHIQI.GWPSE.-272
BsteX    71-GHTLVWHN..QTDSW-83     202-PIHGIGMQAHWSL.NRPTLD-230
BovaI   106-GHCLIWHS..QLAPW-118    227-RIDAIGMQGHIGM.DYPKI.-244
BfibA   139-GHTLVWHS..QTPTW-151    273-VCAGVGMQSHLGTGFP....-288
BfibB    89-GHTLVWHN..QTPKW-101    217-LIDGMGMQSHLLMDHP....-232
CsacA    90-GHTFVWHN..QTPGW-102    213-PIDGIGIQAHWNIWDKNLV.-231
Csac4    42-GHVLVWHN..QTPEW-55     173-LIDGLGLQPTVGLNYPELDS-192
Cfimi   120-GHTLVWHS..QLPDW-132    237-PLDCVGFQSHLIVG...QVP-253
CsteB   120-FHTLVWHN..QTPTG-132    255-PIDGVGHQTHIDI.YNPPV.-272
CtheZ   595-GHTLIWHN..QNPSW-607    714-PIDGVGFQCHFINGMSPEYL-733
CtheX   285-GHTLLWHN..QVPDW-298    415-PISGIGMQMHINI..NSNI.-431
DtheA   107-GHTLVWHN..QTPGW-119    224-PIHGIGIQGHWTL.AWPT..-240
EnidC   105-GHTLVWHS..QLPSW-117    222-PIDGIGSQAHYSS.SHWSS.-239
ErumX   344-GHVLVWHS..QAPEW-356    496-RIDGFGMQGHYSV.NAPTVD-514
PchrP   112-GHTLVWHS..QLPSW-124    230-PIDGIGSQTHLGAGAGAAAS-249
PfluA   342-GHALVWHPSYQLPNW-356    470-PIDGVGFQMHVMNDYPS..I-487
PfluB   384-AHTFVWGA..QSPSW-395    492-YIDAVGLQAH...ELKGMTA-508
RflaA   712-GHTFVWYS..QTPDW-724    846-YIDGIGMQSHLATNYP....-861
TsacA   433-GHTLLWHN..QVPDW-445    563-PIDGIGMQMHINI..NSNI.-579
TaurX    78-GHTLVWWS..QLPPW-90     166-PIIGIGNQTARAAITVWGVA-185
TmarA   448-GHTLVWHN..QTPDW-460    570-LIDGIGMQCHISLA..TDI.-586
TneaA   444-GHTLVWHN..QTPEW-456    566-LIDGIGMQCHISLA..TDI.-582
TbacA   430-GHTLVWHQ..QTPSW-432    559-PVHGVGLQCHISL.DWPDV.-576
```

FIGURE 4: Amino acid alignment of xylanases from family 10. The arrowhead indicates the highly conserved histidines shown in boldface characters (corresponding to H81, H86, and H207 of *S. lividans* mature XlnA). Amino acids are numbered from the translational methionine of each enzyme. Sequence accession numbers from GenBank, SwissProt, or NCBI are indicated in brackets with the following identification key: SlivA, *Streptomyces lividans* XlnA [P26514]; Acti2, *Actimomadura* sp. FC7 XilII [U08894]: AawaA, *Aspergillus awamori* IFO4308 XynA[P33559]; BaccA, *Bacillus* sp. C-125 XynA [P07528]; BsteA, *Bacillus stearothermophilus* T-6 XynA [Z29080]; BsteX, *Bacillus stearothermophilus* 21 Xyn [D28121]; BovaI, *Bacteroides ovatus* V975 XylI [U04957]; BfibA, *Butyrivibrio fibrisolvens* 49 XynA [P23551]; BfibB, *Butyrivibrio fibrisolvens* H17C XynB [P26223]; CsacA, *Caldocellum saccharolyticum* XynA [P23556]; Csac4, *Caldocellum saccharolyticum* ORF4 [P23557]; Cfimi, *Cellulomonas fimi* Cex [P07986]; CsteB, *Clostridium stercorarium* F9 XynB [D12504]; CtheZ, *Clostridium thermocellum* XynZ [P10478]; CtheX, *Clostridium thermocellum* XynX [144776]; DtheA, *Dictyoglomus thermophilum* Rt46B.1 [973983]; EnidC, *Emericella* (*Aspergillus*) *nidulans* XlnC [1050888]; ErumX, *Eubacterium ruminantium* Xln [974180]; PchrP, *Penicillium chrysogenum* Q176 XylP [M98458]; PfluA, *Pseudomonas fluorescens cellulosa* XynA [P14768]; PfluB, *Pseudomonas fluorescens cellulosa* XynB [P23030]; RflaA, *Ruminococcus flavefaciens* XynA [P29126]; TsacA, *Thermoanaerobacter saccharolyticum* B6A-RI XynA [P36917]; TaurX, *Thermoascus aurantiacus* Xyn [P23360]; TmarA, *Thermotoga maritima* XynA [559960]; TneaA, *Thermogota neapolitana* XynA [603892]; TbacA, *Thermophilic bacterium* Rt8.B4A XynA [P40944].

kinetic parameters accurately. Both mutations at H207 (H207K and H207R) affect the k_{cat} of the enzyme, which indicates that the stabilization of the catalytic intermediate of the reaction was affected by the mutation. This effect on the catalytic properties of the enzyme could be due to incorrect positioning of the nucleophile E236 in the catalytic site. Another explanation could be that an adequate stabilization of the catalytic intermediate is prevented by reduced

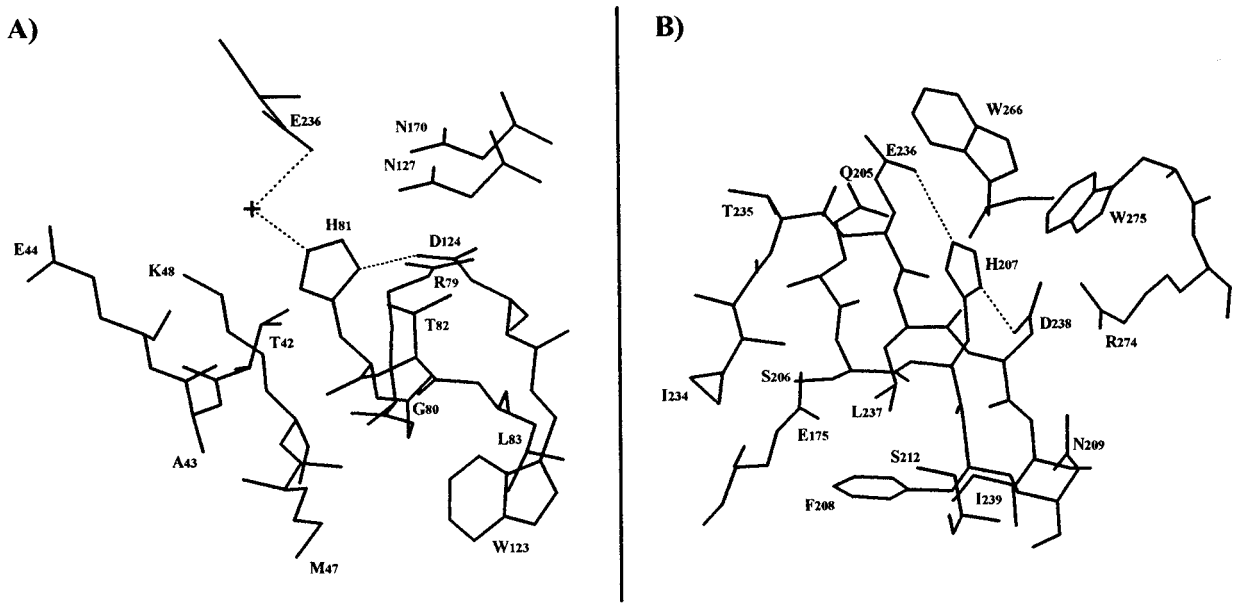

FIGURE 5: Environment of H81 (panel A) and H207 (panel B) of XlnA from *S. lividans* (Derewenda *et al*., 1994). Hydrogen bonds are shown as dashed lines.

interactions between H207 and the nucleophile E236. This is indicated by the change in k_{cat} and is supported by the observation of White *et al*. (*27*), who showed a direct interaction between H205 in Cex from *C. fimi* and the nucleophile E233 in the structure of the covalent enzyme−intermediate complex. Mutation H207K also affects the affinity of the enzyme for birchwood xylan. In this case, a lysine residue at position 207 is likely to disturb the position of other close amino acids interacting with the substrate.

The pH profiles of the specific activity obtained for H207 mutants are all shifted to more acidic values (Figure 1), suggesting that the hydrogen bond between the equivalent of H207 and E236 found in the enzyme−substrate complex (*27*), that is lost upon mutation, is important for the ionization state of the two catalytic residues. However, a comparison of the pH profiles of the apparent k_{cat} of the mutant enzymes with the wild-type gave different results. Comparing the pK_a of the two catalytic residues of the wild-type enzyme with those of the mutants (Table 2), it is apparent that the three mutations modified the hydrogen bond network of the active site such that the pK_a values of the two catalytic residues move toward the theoretical value for free glutamic acid. In fact, the pK_a values of those amino acids are equally affected for mutations H207E and H207R, while the mutation H207K decreases the pK_a of the nucleophile 3 times less than the other mutations did. This would indicate that modification of the hydrogen bonding network in the vicinity of E236 affects interactions involving E128. Thus, the nucleophilicity of E236 might be implicated in maintaining an elevated pK_a for E128 or *vice versa*. Such a dual dependence between two catalytic glutamic acids has been suggested for a family 11 xylanase that uses the same double-displacement mechanism with a similar distance between the two catalytic residues (*25*). Moreover, modeling of the E233D mutant of Cex showed that the absence of hydrogen bonding between H205 and E233 in Cex from *C. fimi* would modify the environment of the active site in a way that could alter the pK_a of both catalytic residues (*28*).

The H207 of XlnA is also important for enzyme stability. All three mutations tested decreased the half-life of the enzyme in the absence of substrate by more than 75%. However, different results were obtained in the presence of substrate. In the presence of xylan, the effect of the mutation on the stability is abolished for mutants H207E and H207R. These two mutants have half-lives similar or slightly lower than the wild-type protein. In both cases, the enzyme is protected by the presence of substrate in the active site against thermal inactivation. For H207K, the 3-fold decrease in affinity for xylan hindered complete stabilization of the enzyme by the substrate. These results suggest the importance of this residue for the hydrogen bond network in the active site of the enzyme.

The large decreases in the concentration of Gdn-HCl necessary to unfold 50% of the xylanases observed for the three mutations at position H207 (Table 3) confirm that the native form of the protein is destabilized by the mutations. On the other hand, in all three cases the *m* value is increased, which is surprising for single point mutations. These increases in *m* values have a greater effect on the ΔG than the differences in transition midpoints resulting in apparent stabilization of the H207 mutant enzymes (Table 3). Similar changes in the *m* value were first reported for the mutated form of staphylococcal nuclease (*29*) and have since been reported for many other proteins (for a list, see ref *30*). Variations of the *m* value were proposed to be the result of modifications in the solvent-accessible surface area of the denatured state (*30*). In the case of XlnA, the increase of the *m* value for the three mutations at position H207 suggests that the mutant proteins have a denatured state with less residual structure than the wild-type protein. H207 is located in a loop, part of the active site, and the integrity of this loop would be essential for the overall stability of the protein. These changes in *m* values suggest that interactions involving H207 could be important for the folding of XlnA.

To study the role of H81 in the structure/function of XlnA, three mutations were made at this position. H81 (Nϵ2) is hydrogen-bonded to E236 (Oϵ1) through a water molecule and is hydrogen-bonded through its Nδ1 atom to D124 (Oδ2) (Figure 5), a highly conserved residue in xylanases from family 10 as shown previously (*14*). Since hydrogen bonding

is involved, H81 was replaced with amino acids that have side chains capable of hydrogen bonding: arginine (H81R), serine (H81S), and tyrosine (H81Y). Mutation at this position destroyed the activity of the enzyme (Table 1). These mutations either affect the positioning of E236 and/or destabilize the intermediate−enzyme complex, slowing down catalysis. Cocrystal structures of xylanases from family 10 with xylopentaose (*4*) and with 2-fluoro-2-deoxy-β-cellobioside, a catalytic intermediate analog (*27*), have shown that the equivalent of H81 is hydrogen-bonded with the 3′-hydroxyl of the saccharide moiety located in subsite E in either cases. Our results suggest that H81 is involved in the stabilization of the catalytic intermediate, since the loss of the hydrogen bond between H81 and the 3′-OH of the saccharide in subsite E causes a large decrease in the k_{cat} of the enzyme. From these results, the importance of H81 for the binding of the substrate cannot be assessed because serine may well replace histidine in the binding to the substrate, while still disrupting the hydrogen bond network of the active site. Earlier, in the case of the H207K mutation, a decrease in affinity for xylan (showed by an increase in the K_M) hindered the protective effect of substrate on the thermal denaturation of the enzyme. Since the three H81 mutants are all fully protected by xylan against thermal denaturation, it is possible that the two other mutations (H81R/Y) do not affect the affinity of the enzyme for xylan. Therefore, the involvement of H81 with the catalytic intermediate seems to be more important than that with the substrate in its ground state, since only the k_{cat} of the enzyme is affected by mutation of this residue. Such a conclusion has been also proposed for N127, an invariant residue in family 10 glycanases located in the active site of XlnA from *S. lividans* (*31*). The equivalent of N127 in Cex from *C. fimi* (N126) was also shown to interact strongly with the 2-hydroxyl of the same saccharide unit as H80 (equivalent of H81 in *S. lividans* XlnA) in the 2-fluoro-2-deoxycellobiosyl−enzyme intermediate crystal structure (*27*). The kinetic results of this study, and other similar results (*31*), support recent results (*32*) that indicate that the interactions of family 10 glycanases with the sugar moieties in subsites D and E are more important for the stabilization of the catalytic intermediate than for the binding of the substrate in its ground state.

The three mutations at position H81 also significantly affect the pH profile of the enzyme (Figure 1). For the specific activity profiles, the effects of the three mutations studied are seen on the acidic side, lowering the apparent pK_a by more than 1 pH unit. In the case of the k_{cat} *vs* pH profiles, the pK_a values of the two catalytic residues are lowered by the mutations, and the nucleophile is the most affected residue. Therefore, in addition to its role in stabilizing the catalytic intermediate, H81 appears to be a very important residue in the hydrogen bond network of the active site, and mutation of this residue modifies the interactions necessary to maintain the ionization state of the two catalytic glutamic acids of XlnA. However, the indirect hydrogen bond between H81 and E236 is probably not directly involved in maintaining the ionization state of the nucleophile since it is not found in the enzyme−substrate complex (*27*).

H81 also plays a key role in enzyme stability, since mutations at this position decrease the half-life of the enzyme by more than 75% (Table 3). However, the stability of the protein compared to that of the wild-type enzyme is restored in the presence of xylan, suggesting that the forces responsible for the binding of substrate have a stabilizing effect on the entire active site hydrogen bond network, thus overcoming the negative effect caused by replacement of H81. The three mutations introduced at position H81 also increase the *m* values of the proteins. Since the transition midpoint of Gdn-HCl denaturation is not affected or only slightly decreased, these mutations increase significantly the free energy of unfolding of the protein [$\Delta G(H_2O)$]. As explained earlier for mutations at position H207, these increases in the *m* values are likely due to losses of residual structure in the denatured state of the mutant proteins and suggest that H81 is involved in important interactions for the native and the denatured state of XlnA.

In conclusion, the results presented in this study show the importance of H81 and H207 for the structure/function of XlnA of *S. lividans*. These two histidine residues are involved in a network of hydrogen bonds which are responsible in maintaining the ionization state of the two catalytic residues responsible for the hydrolysis of β-1,4-glycosidic bond. All six mutations studied at position H81 or H207 lowered the pK_a of E236, which would be of advantage for applications of the enzyme at acidic pH if the activity of the enzyme was maintained. These two histidine residues are also essential for the stability of the protein. These two residues are important in the active site of XlnA and are probably involved in the folding of the native state and the denatured state of the protein.

ACKNOWLEDGMENT

We thank Dr. Joanne Turnbull from Concordia University (Montréal) for use of the CD spectropolarimeter and Dr. Ronald N. McElhany from the University of Alberta (Edmonton) for critical reading of the manuscript. We also thank Lisette Duval for excellent technical assistance.

REFERENCES

1. Henrissat, B., and Bairoch, A. (1993) *Biochem. J. 293*, 781−788.
2. Derewenda, U., Swenson, L., Green, R., Wei, Y., Morosoli, R., Shareck, F., Kluepfel, D., and Derewenda, Z. S. (1994) *J. Biol. Chem. 269*, 20811−20814.
3. White, A., Withers, S. G., Gilkes, N. R., and Rose, D. R. (1994) *Biochemistry 33*, 12546−12552.
4. Harris, G. W., Jenkins, J. A., Connerton, I., Cummings, N., Leggio, L. L., Scott, M., Hazlewood, G. P., Laurie, J. I., Gilbert, H. J., and Pickersgill, R. W. (1994) *Structure 2*, 1107−1116.
5. Dominguez, R., Souchon, H., Spinelli, S., Dauter, Z., Wilson, K. S., Chauvaux, S., Béguin, P., and Alzari, P. M. (1995) *Nat. Struct. Biol. 2*, 569−576.
6. Katsube, Y., Hata, Y., Yamaguchi, H., Moriyama, H., Shinmyo, A., and Okada, H. (1990) in *Protein engineering: Protein design in basic research, medicine, and industry. Proc. 2nd Int. Conf. on Protein Engineering* (Ikehara, M., Ed.) pp 91−96, Japan Scientific Societies Press, Tokyo.
7. Campbell, R. L., Rose, D. R., Wakarchuk, W. W., To, R., Sung, W., and Yaguchi, M. (1993) in *Proceedings of the Second TRICEL symposium on Trichoderma ressei cellulases and other hydrolases* (Suominen, T., and Reinikainen, T., Eds.) pp 63−72, Foundation for biochemical and industrial fermentation research, Helsinki.
8. Törrönen, A., Harkki, A., and Rouvinen, J. (1994) *EMBO J. 13*, 2493−2501.
9. Törrönen, A., and Rouvinen, J. (1995) *Biochemistry 34*, 847−856.

10. Jenkins, J., Leggio, L. L., Harris, G., and Pickersgill, R. (1995) *FEBS Lett. 362*, 281−285.
11. Davies, G., and Henrissat, B. (1995) *Structure 3*, 853−859.
12. Henrissat, B., Callebaut, I., Fabrega, S., Lehn, P., Mornon, J. P., and Davies, G. (1995) *Proc. Natl. Acad. Sci. U.S.A. 92*, 7090−7094.
13. Sinnott, M. L. (1990) *Chem. Rev. 90*, 1171−1202.
14. Moreau, A., Roberge, M., Manin, C., Shareck, F., Kluepfel, D., and Morosoli, R. (1994) *Biochem. J. 302*, 291−295.
15. Kunkel, T. A. (1985) *Proc. Natl. Acad. Sci. U.S.A. 82*, 488−492.
16. Katz, E., Thompson, C. J., and Hopwood, D. A. (1983) *J. Gen. Microbiol. 129*, 2703−2714.
17. Bertrand, J.-L., Morosoli, R., Shareck, F., and Kluepfel, D. (1989) *Biotechnol. Bioeng. 33*, 791−794.
18. Lowry, O. H., Rosebrough, N. J., Farr, A. L., and Randall, R. J. (1951) *J. Biol. Chem. 193*, 265−275.
19. Laemmli, U. K. (1970) *Nature 227*, 680−685.
20. Towbin, H., Staehelin, T., and Gordon, J. (1979) *Proc. Natl. Acad. Sci. U.S.A. 76*, 4350−4354.
21. Lever, M. (1972) *Anal. Biochem. 47*, 273−279.
22. Leatherbarrow, P. J. (1987) Enzfitter, a non-linear regression data analysis program for IBM PC, Elsevier Science Publishers BV., Amsterdam.
23. Leatherbarrow, P. J. (1990) GraFit version 3.0, Erithacus Software Ltd., Staines, U.K.
24. Pace, C. N., Shirley, B. A., and Thomson, J. A. (1989) in *Protein Structure; a practical approach* (Creighton, T. E., Ed.) pp 311−330, IRL Press, Oxford University, England.
25. McIntosh, L. P., Hand, G., Johnson, P. E., Joshi, M. D., Körner, M., Plesniak, L. A., Ziser, L., Wakarchuk, W. W., and Withers, S. G. (1996) *Biochemistry 35*, 9958−9966.
26. Sakon, J., Adney, W. S., Himmel, M. E., Thomas, S. R., and Karplus, P. A. (1996) *Biochemistry 35*, 10648−10660.
27. White, A., Tull, D., Johns, K., Withers, S. G., and Rose, D. R. (1996) *Nat. Struct. Biol. 3*, 149−154.
28. MacLeod, A. M., Tull, D., Rupitz, K., Warren, R. A. J., and Withers, S. G. (1996) *Biochemistry 35*, 13165−13172.
29. Shortle, D., and Meeker, A. K. (1986) *Proteins: Struct., Funct., Genet. 1*, 81−89.
30. Green, S. M., Meeker, A. K., and Shortle, D. (1992) *Biochemistry 31*, 5717−5728.
31. Roberge, M., Dupont, C., Shareck, F., Morosoli, R., and Kluepfel, D. (1997) *Protein Eng.* (in press).
32. Charnock, S. J., Lakey, J. H., Virden, R., Hughes, N., Sinnott, M. L., Hazlewood, G. P., Pickersgill, R., and Gilbert, H. J. (1997) *J. Biol. Chem. 272*, 2942−2951.

BI9703296